


Interfacial materials with special wettability

Tak-Sing Wong, Taolei Sun, Lin Feng, and Joanna Aizenberg, Guest Editors

Various life forms in nature display a high level of adaptability to their environments through the use of sophisticated material interfaces. This is exemplified by numerous biological systems, such as the self-cleaning of lotus leaves, the water-walking abilities of water striders and spiders, the ultra-slipperiness of pitcher plants, the directional liquid adhesion of butterfly wings, and the water collection capabilities of beetles, spider webs, and cacti. The versatile interactions of these natural surfaces with fluids, or special wettability, are enabled by their unique micro/nanoscale surface structures and intrinsic material properties. Many of these biological designs and principles have inspired new classes of functional interfacial materials, which have remarkable potential to solve some of the engineering challenges for industrial and biomedical applications. In this article, we provide a snapshot of the state of the art of biologically inspired materials with special wettability, and discuss some promising future directions for the field.

Introduction

Understanding and controlling wetting—the interaction of fluids with solid surfaces—impacts many areas of science and technology.[1–3] In particular, creating a robust synthetic surface that (1) repels various liquids, (2) allows for directional/switchable fluid manipulation, and/or (3) operates under various environmental conditions would have broad technological implications for areas related to water, energy, and health, but this has proven to be extremely challenging.[4] In nature, many biological surfaces are engineered to have special interfacial interactions with fluids—or special wettability—in order to survive in their innate environments.[5–24] For example, lotus leaves rely on micro- and nanoscale textures to trap a thin layer of air (**Figure 1**a), which then acts as a cushion against liquids and helps to keep the surface clean by carrying away dirt—this is called the lotus effect.[6] Springtails, which are arthropods that live in the soil, have evolved overhanging nanostructured skin patterns (Figure 1b) that help prevent soiling and resist wetting by organic liquids at elevated pressures.[21] *Nepenthes* pitcher plants capture insects with their highly slippery, liquid infused, micro-textured peristome or rim (Figure 1c) without the use of any active prey-capturing mechanisms.[10,25] Central to many of these functional biological surfaces is the presence of unique micro- and nanostructured architectures that allow them to exhibit special wettability. To this end, mimicking these biological surfaces—biomimetics—and learning from these biological concepts—bioinspiration—have led to important advances in the manufacturing and design of synthetic interfacial materials in recent years. This article will highlight state-of-the-art biomimetic and bioinspired materials with special wettability and some of their potential applications.

Biomimetic and bioinspired materials

The maturation of high resolution microscopy techniques, together with rapid advancements in micro- and nanomanufacturing, have enabled scientists and engineers to not only uncover the secrets of functional natural interfacial materials, but also manufacture these functional surfaces using a broad spectrum of synthetic materials. With these collective advances, the field of biomimetics and bioinspiration, particularly the development of interfacial materials, has progressed tremendously during the last decade.[26–28] In the first article in this issue of *MRS Bulletin*, Liu et al. provide a comprehensive overview of recent developments of bioinspired materials with special wettability, ranging from the superior water-walking

Tak-Sing Wong, Department of Mechanical and Nuclear Engineering, The Pennsylvania State University; tswong@psu.edu
Taolei Sun, State Key Laboratory of Advanced Technology for Materials Synthesis and Processing, Wuhan University of Technology, P.R. China; suntl@whut.edu.cn
Lin Feng, Department of Chemistry, Tsinghua University, Beijing, P.R. China; fl@mail.tsinghua.edu.cn
Joanna Aizenberg, School of Engineering and Applied Sciences, Harvard University, Cambridge; jaiz@seas.harvard.edu

DOI: 10.1557/mrs.2013.99

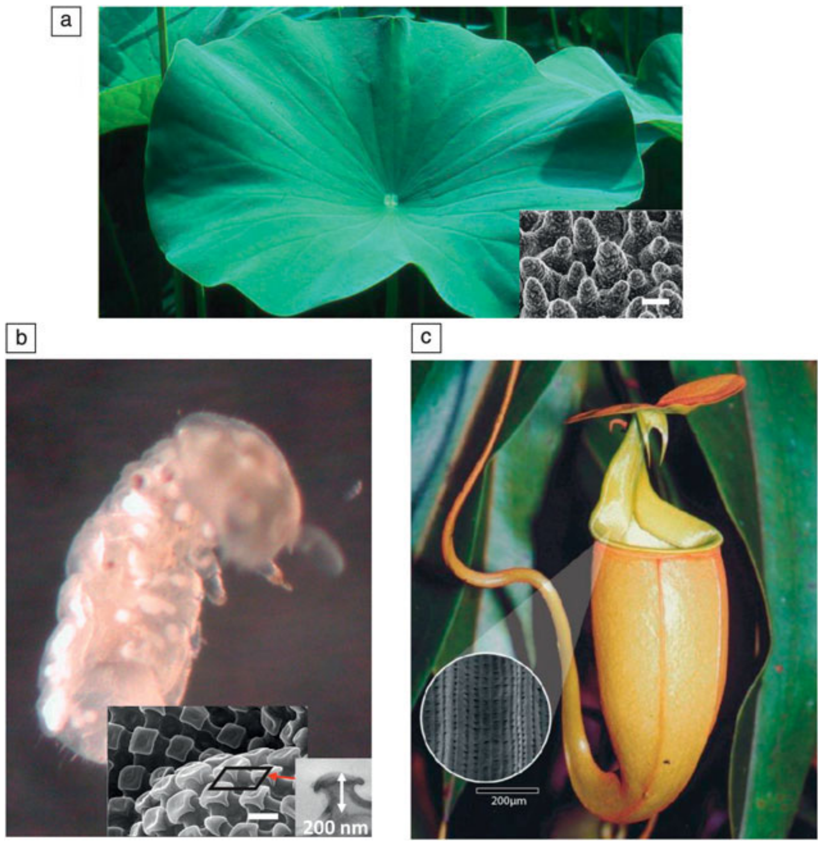

Figure 1. Exemplary liquid-repellent surfaces in nature. (a) A lotus leaf, known for its exceptional water repellency enabled by hierarchical micro/nanostructures (see inset). Scale bar = 10 μm; (b) a springtail, which can resist wetting by organic liquids and at elevated pressures as enabled by overhanging nanostructures (see inset). Scale bar = 500 nm; and (c) a pitcher plant, which utilizes a highly slippery, liquid-infused microstructured peristome or rim to capture prey. Inset shows the microstructures on the peristome. All images are reproduced with permission from the Creative Commons Licenses of References 21 and 93. The pitcher plant image is provided courtesy of W. Federle and H. Bohn.

ability of water striders, the directional adhesion of butterfly wings, the antifogging functionality of mosquito eyes, the water collection of the cactus and spider silk, to the underwater self-cleaning ability of fish scales.

Among these biomimetic studies, the lotus effect has been most widely studied, accounting for >1000 journal papers published in the last decade alone (**Figure 2**). This reflects the remarkable interest and the demand for creating highly liquid-repellent materials. Central to the special wettability of these biomimetic and bioinspired materials is the presence of surface structures at micro- and nanometer scales, which allow them to interact with fluids differently as compared to smooth surfaces. Therefore, it is instructive to look at some of the fundamental theories and terminologies for wetting on structured surfaces.

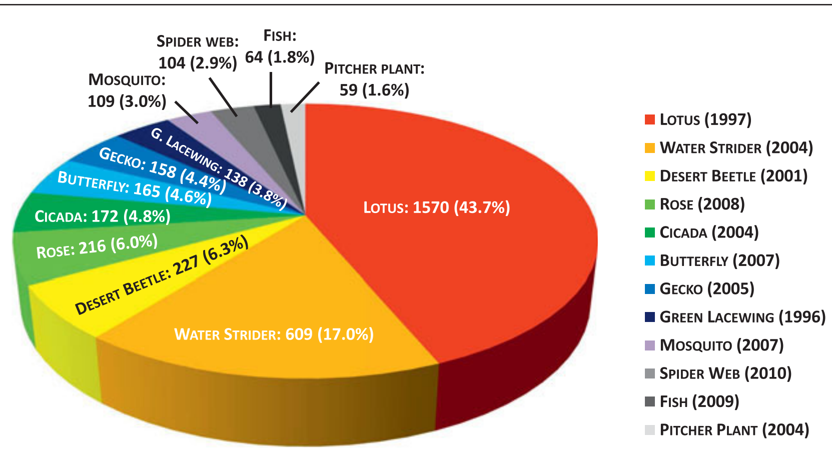

Figure 2. Citations of key papers in biomimicry studies related to interfacial materials with special wettability from 2002 to 2012. Citation data are obtained from ISI Web of Knowledge provided by Thomson Reuters.[5,6,8,10–12,14,16–20]

Wetting on structured surfaces

When a liquid droplet is deposited on a smooth solid surface in air, three distinctive interfacial boundaries arise that intersect at a well-defined contact angle, θ (**Figure 3**a). Competition among the adhesion forces of the liquid, vapor, and solid surfaces results in a force equilibrium at the three-phase contact line,[29] which can be described by Young's equation:

$$\gamma_{LV} \cos\theta = \gamma_{SV} - \gamma_{SL}, \qquad (1)$$

where γ_{LV}, γ_{SV}, and γ_{SL} are the surface tensions for liquid-vapor, solid-vapor, and solid-liquid interfaces, respectively, and θ is the intrinsic contact angle at the three-phase contact line. By convention, if $\theta \geq 90°$, the solid is said to "hate" the fluid droplet (hydrophobic for the case of water). Likewise, if $\theta < 90°$, the solid is said to "like" the fluid droplet (hydrophilic for the case of water).

However, real surfaces are rarely smooth. The contact angles of liquid droplets observed (or apparent contact angles, θ^*) (see Figure 3b) on these real surfaces typically deviate significantly from those described by Young's equation. Wetting of liquid droplets on structured surfaces can be roughly described by two distinct modes. In the first mode, the liquid closely follows the topography of the surface, forming a continuous liquid-solid interface (Figure 3b). The apparent contact angle can be described by the Wenzel equation developed in 1936:

$$\cos\theta^* = r \cos\theta, \qquad (2)$$

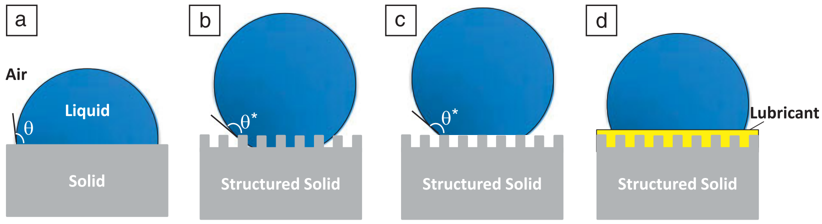

Figure 3. Wetting on smooth and structured surfaces. A liquid droplet sitting on (a) a smooth surface with an intrinsic contact angle, θ; (b) a textured surface that is completely wetted by the liquid, known as a Wenzel state droplet; (c) a textured surface with trapped air pockets, known as a Cassie state droplet; and (d) a textured surface that is infused with an immiscible lubricating fluid (or slippery liquid-infused porous surfaces). Note: θ*, apparent contact angle.

where r is the roughness factor, defined as the ratio of the actual surface area and the projected surface area of the solid.[30] The Wenzel equation indicates that roughness can amplify the wettability of a solid. For example, if the solid is intrinsically hydrophobic, roughness will further enhance the surface hydrophobicity.

In the second mode, the liquid does not follow the topography of the solid surface; instead the liquid is suspended on a mixed interface composed of surface protrusions with air pockets trapped between them (Figure 3c). The apparent contact angle in this mode was first described by the Cassie–Baxter equation in 1944[31] and was further extended by Cassie to heterogeneous surfaces in 1948,[32]

$$\cos\theta^* = A_1\cos\theta_1 + A_2\cos\theta_2, \tag{3}$$

where A_1 and A_2 are surface area fractions (i.e., $A_1 + A_2 = 1$), and θ_1 and θ_2 are the intrinsic contact angles of materials 1 and 2, respectively. The Cassie equation indicates that to achieve a perfect non-wetting situation (i.e., $\theta^* \sim 180°$), one needs to maximize the area fraction of the air pockets trapped beneath the liquid droplet. The concept put forth by Cassie and Baxter explained the large contact angles observed in many plant and animal surfaces, such as the lotus leaf.[33] In addition to the surface area concept model proposed by Cassie and Baxter, recent experimental and theoretical studies have highlighted the importance of the three-phase contact lines at the edges of the surface protrusions to macroscopic wettability.[34–38] In particular, the interactions of the liquid contact line with the surface protrusions become important (i.e., pinning) when the liquids are in motion on these structured surfaces.

Achieving a high apparent contact angle can reduce the normal adhesion of a liquid droplet to the solid surface due to a reduction of the liquid-solid contact area. However, contact angle alone does not quantify the resistance to liquid motion in the direction tangential to the surface.[34,39–41] In particular, liquids sitting on rough surfaces exhibit a variety of contact angles bounded by two extreme values due to pinning. The upper limit is known as the advancing contact angle, θ_A, whereas the lower limit is referred to as the receding contact angle, θ_R. The difference between these values is known as contact angle hysteresis, $\Delta\theta$, whose physical origin is attributed to pinning of the liquid contact line on the nanoscopic surface roughness.[42–45] The presence of the contact angle hysteresis gives rise to a surface retention force, F_R, that resists the motion of a liquid droplet of a characteristic length, L,[40]

$$F_R = \gamma_{LV} L(\cos\theta_R - \cos\theta_A). \tag{4}$$

Therefore, minimizing the hysteresis is the key to minimizing resistance to motion, resulting in high mobility of the droplets and therefore in significantly improved liquid-repellency of the surface.

By convention, we describe a material as superhydrophobic if it displays an apparent contact angle for water of ≥ 150° with a contact angle hysteresis ≤ 5–10°. If the material displays similar values with oils, we describe the surface as superoleophobic. If the material meets these criteria for both water and oils, we term the material superomniphobic or superamphiphobic (**Table I**).

Extreme fluid repellency

Lotus leaves have an exceptional ability to repel water but not oils; therefore, this natural material is only superhydrophobic. After more than a decade of research and development, we now have many different ways to create synthetic superhydrophobic surfaces,[46–49] but creating materials that are both superhydrophobic and superoleophobic (i.e., superomniphobic) based on the lotus-leaf model has proven more difficult. A fundamental reason for this is that oils have intrinsically low surface tension, which makes them prone to wet the micro/nanoscopic surface textures more readily than liquids of higher surface tension, thereby displacing the air pockets trapped in between the surface textures and leading to significant liquid pinning.

Despite the challenges, recent efforts have shown that by carefully engineering surface textures with overhanging

Table I. Classification of liquid-repellent states.

State	Superhydrophobic	Superoleophobic	Omniphobic	Superomniphobic/ Superamphiphobic
Liquids	Water	Oils	Water & Oils	Water & Oils
θ* (°)	≥ 150°	≥ 150°	< 150°	≥ 150°
Δθ* (°)	≤ 5–10°	≤ 5–10°	≤ 5–10°	≤ 5–10°

Note: θ*, apparent contact angle; Δθ*, apparent contact angle hysteresis.

features, it is possible to create superomniphobic materials that can repel both water and oils.[50–53] The novelty behind these surfaces is the creation of convex topography (or re-entrant curvatures) such that droplet pinning at the edges of the micro/nanoscopic overhanging structures prevents further penetration. This development has further advanced the capabilities of lotus leaf-inspired surfaces to repel not only water, but also a much broader range of fluids.[54] In the second article in this issue, Kota et al. discuss recent advances in superomniphobic surfaces and their durability issues. It is interesting to note that springtails also possess similar overhanging nanoscale textured patterns to protect themselves from soiling (Figure 1b).[21] These natural surfaces were shown to resist wetting by many organic liquids and at elevated pressures, and demonstrate a number of similarities to their artificial counterparts, which will be described in the article by Kota et al.[50–52,54]

Anisotropic fluid repellency

In addition to lotus leaves, which display a high level of omnidirectional water repellency, a number of biological surfaces are able to shed water only in a specific direction—known as anisotropic wetting. For example, the wings of butterflies can shed water droplets easily along the radial outward direction away from their wings, but not in the opposite direction.[17] The legs of water striders are covered with tiny oriented hairs with fine nanogrooves that allow them to propel the strider efficiently on water surfaces.[11,55] Another example can be found on rice leaves that consist of one-dimensional arrays of oriented micro/nanotextures that enable the transport of water droplets in a particular direction.[9] Central to these biological surfaces are the orientations and arrangements of the surface textures that provide precise control over the direction of droplet motion. Inspirations from these natural anisotropic surfaces have led to artificial surfaces that display similar anisotropic wetting behaviors.[56–58] In the third article in this issue, Hancock and Demirel summarize recent experimental and theoretical progress in the design, synthesis, and characterization of engineered surfaces that demonstrate anisotropic wetting properties, as well as their potential applications.

Toward industrial applications in extreme environments

In addition to fundamental research, important advances have been made in understanding how these materials could be utilized in various applications under different environmental conditions, particularly in industrial processes that involve phase changes such as condensation[59–63] and icing.[64–71] On one hand, for instance, vapor condensation is commonly encountered in power generation, thermal management, and desalination plants. On the other hand, ice formation and accretion present serious economic and safety issues for essential infrastructure such as aircraft, power lines, wind turbines, and commercial and residential refrigeration. Passive coatings that can effectively remove condensed vapor and/or reduce ice adhesion are thus critically needed. In the fourth article in this issue, recent developments in the use of superhydrophobic surfaces for condensation control are discussed by Miljkovic and Wang from an academic research perspective. In the last article of the issue, Alizadeh et al. discuss how some of these bioinspired materials can contribute to the effective removal of condensed vapor and ice from an industrial viewpoint.

Outlook

One of the ultimate goals in the field of bioinspired interfacial materials is to create a robust, scalable, and low-cost surface that can repel any fluid, self-heal upon damage, allow for smart/switchable control of wettability, and operate under a wide range of environmental conditions, such as extreme temperatures, high pressures, and harsh chemicals. As discussed here, cutting-edge development of synthetic liquid-repellent surfaces has primarily been modeled after the lotus effect, with many important advances made over the last decade (**Figure 4**). Some of these lotus leaf-inspired surfaces have been designed to repel both aqueous and organic liquids,[50–54] others can be manufactured from low-cost (such as plastics)[72] or mechanically robust (such as ceramic) materials,[73] yet another set of studies demonstrated switchable wettability,[13,74–77] partial self-healing capability,[78–80] or the ability to operate under

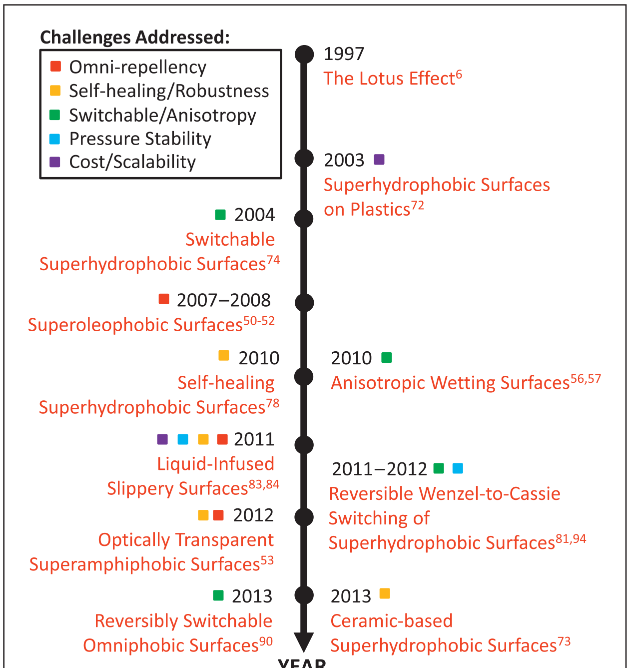

Figure 4. Timeline of key materials innovations and developments in bioinspired liquid-repellent surfaces in the past decade (2003–2013).[6,50–53,56,57,72–74,78,81,83,84,90,94] Note that this timeline only covers material development and does not include the key fundamental theoretical/computational/experimental discoveries during the period. Readers are referred to recent reviews by Quéré,[4] Marmur,[95] Nosonovsky and Bhushan,[96] and Bormashenko.[97]

Table II. A comparison matrix between the performance of SLIPS (slippery liquid-infused porous surfaces) and the best available parameters of the lotus leaf-inspired superhydrophobic surfaces published in the literature.

Technology	Contact Angle Hysteresis (°)	Dynamic Pressure (Pa)	Static Pressure (Pa)	Self-Healing (sec)	Ice Adhesion (kPa)
SLIPS	< 2.5°[83] (water & oils)	> ~5000[83] (water & oils)	~6.85×10^{7} [83] (water & oils)	~0.15[83]	~15[88]
Lotus leaf-inspired surfaces	~10°–30° (oils)[52] <5° (water)[52]	~1000[53] (oils) > ~5000[98] (water)	~7×10^{5} (water)[81]	~180[79]	~Order of 100 or above[66]

moderate pressure (up to ~7 atm or ~7×10^{5} Pa).[81] However, these impressive properties, where present, have been demonstrated separately on different materials, rather than integrated into a single material. Thus many of these surfaces face severe limitations to their practical applications: they show limited oleophobicity with high contact angle hysteresis; fail under high pressure[82] and upon any physical damage; and/or cannot completely self-heal.

Very recently, a conceptually different approach to creating liquid-repellent materials—inspired by the slippery *Nepenthes* pitcher plants[10]—was developed[83] that may potentially address many of the challenges found in the lotus leaf-inspired surfaces (**Table II**). The new material consists of a continuous film of lubricating liquid locked in place by a micro/nanostructured substrate (Figure 3d), and is termed slippery liquid-infused porous surfaces (SLIPS),[83] or slippery pre-suffused surfaces[84] or lubricant-impregnated surfaces.[85,86] The liquid-infused structured surface outperforms its natural counterparts and state-of-the-art synthetic surfaces in its ability to repel various simple and complex liquids (water, crude oil, and blood); maintain low contact angle hysteresis (<2.5°); rapidly restore liquid-repellency after physical damage (within 0.1–1 s); function at high pressures (up to ~676 atm or ~6.85×10^{7} Pa); resist bacterial bio-fouling[87] and ice adhesion;[88,89] enhance condensation;[85] and switch wettability in response to mechanical stimuli[90] (see Table II). Since these properties can all be incorporated into a single coating, new approaches of forming such coatings on a broad variety of materials, such as metals, ceramics, or polymers, are being developed.[91] The slippery surfaces can potentially be used in a wide variety of industrial and medical applications and environments and may provide alternative solutions for designing materials with special wettability that could not be addressed by conventional lotus leaf-inspired surfaces.[92]

Ultimately, the widespread application of any of the aforementioned bioinspired interfacial materials is dictated by their cost, scalability, and robustness, which are important for their practical use on a large scale and accessibility to people with low budgets and around the world. While promising results have been demonstrated for many of these bioinspired materials, continuing research is necessary to bring down the material and fabrication costs, as well as to enhance their longevity and robustness without compromising functional performance.

Acknowledgments

The authors would like to thank Alison Grinthal for help with manuscript preparation. J.A. and T.S.W. would also like to acknowledge funding support by the Office of Naval Research MURI Grant under Award No. N00014–12–1-0875.

References

1. P.G. de Gennes, *Rev. Mod. Phys.* **57**, 827 (1985).
2. P.G. de Gennes, F. Brochard-Wyart, D. Quere, *Capillarity and Wetting Phenomena : Drops, Bubbles, Pearls, Waves* (Springer, New York, 2004).
3. Y. Pomeau, E. Villermaux, *Phys. Today* **59**, 39 (2006).
4. D. Quéré, *Annu. Rev. Mater. Res.* **38**, 71 (2008).
5. T. Wagner, C. Neinhuis, W. Barthlott, *Acta Zool.* **77**, 213 (1996).
6. W. Barthlott, C. Neinhuis, *Planta* **202**, 1 (1997).
7. C. Neinhuis, W. Barthlott, *Ann. Bot.* **79**, 667 (1997).
8. A.R. Parker, C.R. Lawrence, *Nature* **414**, 33 (2001).
9. L. Feng, S. Li, Y. Li, H. Li, L. Zhang, J. Zhai, Y. Song, B. Liu, L. Jiang, D. Zhu, *Adv. Mater.* **14**, 1857 (2002).
10. H.F. Bohn, W. Federle, *Proc. Natl. Acad. Sci. U.S.A.* **101**, 14138 (2004).
11. X.F. Gao, L. Jiang, *Nature* **432**, 36 (2004).
12. W. Lee, M.-K. Jin, W.-C. Yoo, J.-K. Lee, *Langmuir* **20**, 7665 (2004).
13. T.L. Sun, L. Feng, X.F. Gao, L. Jiang, *Acc. Chem. Res.* **38**, 644 (2005).
14. W.R. Hansen, K. Autumn, *Proc. Natl. Acad. Sci. U.S.A.* **102**, 385 (2005).
15. D.L. Hu, J.W.M. Bush, *Nature* **437**, 733 (2005).
16. X. Gao, X. Yan, X. Yao, L. Xu, K. Zhang, J. Zhang, B. Yang, L. Jiang, *Adv. Mater.* **19**, 2213 (2007).
17. Y. Zheng, X. Gao, L. Jiang, *Soft Matter* **3**, 178 (2007).
18. L. Feng, Y. Zhang, J. Xi, Y. Zhu, N. Wang, F. Xia, L. Jiang, *Langmuir* **24**, 4114 (2008).
19. M.J. Liu, S.T. Wang, Z.X. Wei, Y.L. Song, L. Jiang, *Adv. Mater.* **21**, 665 (2009).
20. Y. Zheng, H. Bai, Z. Huang, X. Tian, F.-Q. Nie, Y. Zhao, J. Zhai, L. Jiang, *Nature* **463**, 640 (2010).
21. R. Helbig, J. Nickerl, C. Neinhuis, C. Werner, *PloS One* **6**, (2011).
22. N.J. Mlot, C.A. Tovey, D.L. Hu, *Proc. Natl. Acad. Sci. U.S.A.* **108**, 7669 (2011).
23. C. Duprat, S. Protiere, A.Y. Beebe, H.A. Stone, *Nature* **482**, 510 (2012).
24. J. Ju, Y. Zheng, T. Zhao, R. Fang, L. Jiang, *Nat. Commun.* **3**, 1247 (2012).
25. Y. Forterre, J.M. Skotheim, J. Dumais, L. Mahadevan, *Nature* **433**, 421 (2005).
26. N.F. Lepora, P. Verschure, T.J. Prescott, *Bioinspir. Biomim.* **8**, (2013).
27. J. Genzer, A. Marmur, *MRS Bull.* **33**, 742 (2008).
28. B. Bhushan, *Philos. Trans. R. Soc. London, Ser. A* **367**, 1445 (2009).
29. T. Young, *Philos. Trans. R. Soc. London* **95**, 65 (1805).
30. R.N. Wenzel, *Ind. Eng. Chem.* **28**, 988 (1936).
31. A.B.D. Cassie, S. Baxter, *Trans. Faraday Soc.* **40**, 0546 (1944).
32. A.B.D. Cassie, *Discuss. Faraday Soc.* **3**, 11 (1948).
33. A.B.D. Cassie, S. Baxter, *Nature* **155**, 21 (1945).
34. D. Oner, T.J. McCarthy, *Langmuir* **16**, 7777 (2000).
35. C.W. Extrand, *Langmuir* **20**, 5013 (2004).
36. C. Dorrer, J. Ruhe, *Langmuir* **22**, 7652 (2006).
37. T.S. Wong, C.M. Ho, *Langmuir* **25**, 12851 (2009).
38. E. Bormashenko, *J. Colloid Interface Sci.* **360**, 317 (2011).
39. R.H. Dettre, R.E. Johnson, *J. Phys. Chem.* **69**, 1507 (1965).
40. C.G. Furmidge, *J. Colloid Sci.* **17**, 309 (1962).
41. W. Chen, A.Y. Fadeev, M.C. Hsieh, D. Öner, J. Youngblood, T.J. McCarthy, *Langmuir* **15**, 3395 (1999).
42. J.W. Gibbs, *The Scientific Papers of J. Willard Gibbs* (Dover Publications, New York, 1961).
43. J.F. Oliver, C. Huh, S.G. Mason, *J. Colloid Interface Sci.* **59**, 568 (1977).
44. T. Ondarcuhu, A. Piednoir, *Nano Lett.* **5**, 1744 (2005).
45. T.S. Wong, A.P.H. Huang, C.M. Ho, *Langmuir* **25**, 6599 (2009).
46. D. Quere, *Rep. Prog. Phys.* **68**, 2495 (2005).
47. X.M. Li, D. Reinhoudt, M. Crego-Calama, *Chem. Soc. Rev.* **36**, 135 (2007).
48. P. Roach, N.J. Shirtcliffe, M.I. Newton, *Soft Matter* **4**, 224 (2008).
49. C. Dorrer, J. Ruhe, *Soft Matter* **5**, 51 (2009).

50. A. Tuteja, W. Choi, M. Ma, J.M. Mabry, S.A. Mazzella, G.C. Rutledge, G.H. McKinley, R.E. Cohen, *Science* **318**, 1618 (2007).
51. A. Ahuja, J.A. Taylor, V. Lifton, A.A. Sidorenko, T.R. Salamon, E.J. Lobaton, R. Kolodner, T.N. Krupenkin, *Langmuir* **24**, 9 (2008).
52. A. Tuteja, W. Choi, J.M. Mabry, G.H. McKinley, R.E. Cohen, *Proc. Natl. Acad. Sci. U.S.A.* **105**, 18200 (2008).
53. X. Deng, L. Mammen, H.J. Butt, D. Vollmer, *Science* **335**, 67 (2012).
54. S. Pan, A.K. Kota, J.M. Mabry, A. Tuteja, *J. Am. Chem. Soc.* **135**, 578 (2013).
55. D.L. Hu, B. Chan, J.W.M. Bush, *Nature* **424**, 663 (2003).
56. K.H. Chu, R. Xiao, E.N. Wang, *Nat. Mater.* **9**, 413 (2010).
57. N.A. Malvadkar, M.J. Hancock, K. Sekeroglu, W.J. Dressick, M.C. Demirel, *Nat. Mater.* **9**, 1023 (2010).
58. M.J. Hancock, K. Sekeroglu, M.C. Demirel, *Adv. Funct. Mater.* **22**, 2223 (2012).
59. C.H. Chen, Q. Cai, C. Tsai, C.-L. Chen, G. Xiong, Y. Yu, Z. Ren, *Appl. Phys. Lett.* **90**, 173108 (2007).
60. J.B. Boreyko, C.H. Chen, *Phys. Rev. Lett.* **103**, 184501 (2009).
61. R. Enright, N. Miljkovic, A. Al-Obeidi, C.V. Thompson, E.N. Wang, *Langmuir* **28**, 14424 (2012).
62. N. Miljkovic, R. Enright, E.N. Wang, *ACS Nano* **6**, 1776 (2012).
63. N. Miljkovic, R. Enright, Y. Nam, K. Lopez, N. Dou, J. Sack, E.N. Wang, *Nano Lett.* **13**, 179 (2013).
64. L.L. Cao, A.K. Jones, V.K. Sikka, J.Z. Wu, D. Gao, *Langmuir* **25**, 12444 (2009).
65. S.A. Kulinich, M. Farzaneh, *Appl. Surf. Sci.* **255**, 8153 (2009).
66. A.J. Meuler, J.D. Smith, K.K. Varanasi, J.M. Mabry, G.H. McKinley, R.E. Cohen, *ACS Appl. Mater. Interfaces* **2**, 3100 (2010).
67. L. Mishchenko, B. Hatton, V. Bahadur, J.A. Taylor, T. Krupenkin, J. Aizenberg, *ACS Nano* **4**, 7699 (2010).
68. K.K. Varanasi, T. Deng, J.D. Smith, M. Hsu, N. Bhate, *Appl. Phys. Lett.* **97**, 234102 (2010).
69. M. He, J. Wang, H. Li, X. Jin, J. Wang, B. Liu, Y. Song, *Soft Matter* **6**, 2396 (2010).
70. S.A. Kulinich, S. Farhadi, K. Nose, X.W. Du, *Langmuir* **27**, 25 (2011).
71. V. Bahadur, L. Mishchenko, B. Hatton, J.A. Taylor, J. Aizenberg, T. Krupenkin, *Langmuir* **27**, 14143 (2011).
72. H.Y. Erbil, A.L. Demirel, Y. Avci, O. Mert, *Science* **299**, 1377 (2003).
73. G. Azimi, R. Dhiman, H.-M. Kwon, A.T. Paxson, K.K. Varanasi, *Nat. Mater.* **12**, 315 (2013).
74. T. Sun, G. Wang, L. Feng, B. Liu, Y. Ma, L. Jiang, D. Zhu, *Angew. Chem. Int. Ed.* **43**, 357 (2004).
75. A. Sidorenko, T. Krupenkin, A. Taylor, P. Fratzl, J. Aizenberg, *Science* **315**, 487 (2007).
76. A. Sidorenko, T. Krupenkin, J. Aizenberg, *J. Mater. Chem.* **18**, 3841 (2008).
77. A. Grigoryev, T. Tokarey, K.G. Kornev, I. Luzinov, S. Minko, *J. Am. Chem. Soc.* **134**, 12916 (2012).
78. Y. Li, L. Li, J.Q. Sun, *Angew. Chem. Int. Ed.* **49**, 6129 (2010).
79. H. Wang, Y. Xue, J. Ding, L. Feng, X. Wang, T. Lin, *Angew. Chem.* **50**, 11433 (2011).
80. X.L. Wang, X.J. Liu, F. Zhou, W.M. Liu, *Chem. Commun.* **47**, 2324 (2011).
81. C. Lee, C.J. Kim, *Phys. Rev. Lett.* **106**, 014502 (2011).
82. R. Poetes, K. Holtzmann, K. Franze, U. Steiner, *Phys. Rev. Lett.* **105**, 166104 (2010).
83. T.S. Wong, S.H. Kang, S.K.Y. Tang, E.J. Smythe, B.D. Hatton, A. Grinthal, J. Aizenberg, *Nature* **477**, 443 (2011).
84. A. Lafuma, D. Quere, *Europhys. Lett.* **96**, 56001 (2011).
85. S. Anand, A.T. Paxson, R. Dhiman, J.D. Smith, K.K. Varanasi, *ACS Nano* **6**, 10122 (2012).
86. J.D. Smith, R. Dhiman, S. Anand, E. Reza-Garduno, R.E. Cohen, G.H. McKinley, K.K. Varanasi, *Soft Matter* **9**, 1772 (2013).
87. A.K. Epstein, T.S. Wong, R.A. Belisle, E.M. Boggs, J. Aizenberg, *Proc. Natl. Acad. Sci. U.S.A.* **109**, 13182 (2012).
88. P. Kim, T.S. Wong, J. Alvarenga, M.J. Kreder, W.E. Adorno-Martinez, J. Aizenberg, *ACS Nano* **6**, 6569 (2012).
89. H.A. Stone, *ACS Nano* **6**, 6536 (2012).
90. X. Yao, Y. Hu, A. Grinthal, T.S. Wong, L. Mahadevan, J. Aizenberg, *Nat. Mater.*, doi: 10.1038/NMAT3598 (2013).
91. P. Kim, M.J. Kreder, J. Alvarenga, J. Aizenberg, *Nano Lett.* **13**, 1793 (2013).
92. M. Nosonovsky, *Nature* **477**, 412 (2011).
93. H.J. Ensikat, P. Ditsche-Kuru, C. Neinhuis, W. Barthlott, *Beilstein J. Nanotechnol.* **2**, 152 (2011).
94. T. Verho, J.T. Korhonen, L. Sainiemi, V. Jokinen, C. Bower, K. Franze, S. Franssila, P. Andrew, O. Ikkala, R.H.A. Ras, *Proc. Natl. Acad. Sci. U.S.A.* **109**, 10210 (2012).
95. A. Marmur, *Annu. Rev. Mater. Res.* **39**, 473 (2009).
96. M. Nosonovsky, B. Bhushan, *Curr. Opin. Colloid Interface Sci.* **14**, 270 (2009).
97. E. Bormashenko, *Philos. Trans. R. Soc. London, Ser. A* **368**, 4695 (2010).
98. T.P.N. Nguyen, P. Brunet, Y. Coffinier, R. Boukherroub, *Langmuir* **26**, 18369 (2010). □